

Self-Supervised Learning for Invariant Representations from Multi-Spectral and SAR Images

Pallavi Jain, Bianca Schoen-Phelan, Robert Ross

School of Computer Science

Technological University Dublin

Dublin, Ireland

{pallavi.jain, bianca.schoenphelan, robert.ross}@tudublin.ie

Abstract—Self-Supervised learning (SSL) has become the new state-of-art in several domain classification and segmentation tasks. Of these, one popular category in SSL is distillation networks such as BYOL. This work proposes RSDnet, which applies the distillation network (BYOL) in the remote sensing (RS) domain where data is non-trivially different from natural RGB images. Since Multi-spectral (MS) and synthetic aperture radar (SAR) sensors provide varied spectral and spatial resolution information, we utilised them as an implicit augmentation to learn invariant feature embeddings. In order to learn RS based invariant features with SSL, we trained RSDnet in two ways, i.e., single channel feature learning and three channel feature learning. This work explores the usefulness of single channel feature learning from random MS and SAR bands compared to the common notion of using three or more bands. In our linear evaluation, these single channel features reached a 0.92 F1 score on the EuroSAT classification task and 59.6 mIoU on the DFC segmentation task for certain single bands. We also compared our results with ImageNet weights and showed that the RS based SSL model outperforms the supervised ImageNet based model. We further explored the usefulness of multi-modal data compared to single modality data, and it is shown that utilising MS and SAR data learn better invariant representations than utilising only MS data.

Index Terms—self-supervised learning, unsupervised learning, satellite images, optical-sar fusion

I. INTRODUCTION

Computer vision applications to satellite imagery have progressed tremendously over recent years with the availability of multi-modal imagery. Nevertheless, the remote sensing (RS) community faces two major problems: labelled data scarcity and, secondly, dealing with the multi-sensor and multi-modal nature of data obtained from different satellites.

Primarily, satellites are broadly divided into Optical and Synthetic Aperture Radar (SAR) sensors. On the one hand, optical sensors provide easy to read information and vary in spectral and spatial resolution levels but are impacted negatively by weather conditions like clouds. On the other hand, SAR sensors provide high resolution and weather independent data but do not provide readily interpretable images. As both have their benefits, several research efforts have shown the possibility of combining the data from these two sensors to obtain better quality information [1]. Learning features from both modalities has also shown significant advantages in previous works [2]–[4].

Although raw satellite data is freely available, leveraging a large amount of labelled data remains a challenge due

to the expense of human annotation and domain expertise [5]. To address this problem, transfer learning is one of the solutions which we can leverage from the machine learning community. This, in fact, has shown excellent generalisation capability in several domains [6]–[8]. Unfortunately, however, most ML pre-trained models are based on RGB and non-RS images, which are different in spectral and spatial aspects from satellite images. This problem has motivated many RS domain researchers to either obtain a large amount of labelled land cover data and pre-train a supervised model, or to apply self-supervised learning to the RS data. With the challenges associated with labelled data, self-supervised learning has become quite popular in the RS community [3], [4], [9]–[11].

In recent years, self-supervised learning (SSL) has shown competitive results compared to supervised learning. SSL can be broadly divided into three categories: pre-text task learning, contrastive learning, and distillation networks. Pre-text task (PTT) learning is based on proxy task prediction such as rotation prediction, solving jigsaw puzzles, colourisation, etc. [12]–[14]. Although PTT learning has shown great advantages in learning different invariant properties, such as rough boundaries and semantic information about the images, it does not generalise well in latter layers of the network [15]. Meanwhile, contrastive learning involves the use of positive and negative pairs of images such as in SimCLR [16] or MoCo [17]. This usually leads to an increase in the need for memory requirements and increases in the computational cost as they depend on a high batch size for the contrastive approach to be most effective. Recently, distillation networks such as BYOL [18] and DINO [19] have shown the potential of using only positive pairs to learn better representations, which ultimately reduced the need for a large batch size in comparison to other contrastive learning approaches. Although these methods have claimed to add several factors to models that should prevent the common collapse problem in siamese networks, this is still an active area of research.

In SSL type learning, apart from network architectures, the design of data augmentation such as random crops, random rotation, colour jitters, random greyscale etc., is a crucial part of the learning process. The goal of distillation networks such as BYOL is to learn invariant feature embedding by bringing these augmented views closer. We argue that having the use of multi-modal satellite data can provide implicit augmentation to the model when we utilise MS and SAR data as augmented pairs of images. Motivated by this, we trained

a remote sensing-based SSL distillation network (RSDnet) against the MS and SAR data to learn invariant spectral and spatial features. Although both data sources vary in terms of resolution and modality, our hypothesis is that feature-level information should remain the same and provide valid inputs to the distillation network process.

In summary, the main contributions of this work are then as follows:

- We investigated the importance of having RS based pre-trained models compared to traditional RGB or Non-RS based pre-trained models. For this, we compared our BYOL based RSDnets weights with popular ImageNet and MS COCO pre-trained weights. We also compared our results with another RS-based contrastive learning model SeCo [20]. This further investigates the suitability of self-supervised distillation networks for RS-based learning.
- We explored the usefulness of multi-modality for feature learning rather than learning by a single modality. For that, we trained RSDnet with MS-SAR data and, also, with only MS data, which further confirmed the effectiveness of learning invariant features from MS-SAR data.
- Finally, we also validate single band feature learning efficiency against three band feature learning in satellite imaging. In general, each MS band has its own reflectance property to differentiate between geographical features such as water, land cover and more. This motivated us to explore single-band invariant feature learning, which we believe can learn powerful features through a model combining three or more bands.

II. RELATED WORK

This section discusses relevant previous work in self-supervised learning and its application in the remote sensing domain.

A. Contrastive Learning and Distillation Networks

Self-supervised learning (SSL) performance has closed the gap with supervised learning [18], [19], which has helped solve the big problem of labelled data requirements for deep learning.

Many contrastive and distillation networks have been proposed with increasing interest and performance enhancements. These networks are based on the general class of siamese networks, which learn feature embedding based on the similarity between two images. Unfortunately, the early siamese networks commonly suffered from model collapse to trivial solutions. However, with careful control over the input data, model architecture, and loss function, contrastive and distillation network approaches have been able to avoid this collapse.

Contrastive learning such as SimCLR [16] deal with positive and negative pairs of images intending to maximise the agreement in projections between similar images while minimising for dissimilar images. Similarly, MoCo [17] leverages the concept of a momentum encoder and memory bank for negative feature vectors. Although these learning methods show good performance, they are computationally costly due to the use

of negative pairs that require large batch size and memory requirements.

Meanwhile, distillation networks such as BYOL [18], and DINO [19] utilise only positive pairs and have become quite popular in terms of performance and memory efficiency. BYOL and DINO are similarity-based networks whose architecture is inspired by concepts from MoCo [17] and follows a student-teacher approach. Here, teacher encoders do not have error-signal backpropagation; instead, they utilise slow moving averages from the student network weights. This makes them asymmetric and prevents embeddings from collapsing.

In addition to contrastive and distillation networks, Barlow Twin (BT) [21] has been proposed which employs a redundancy reduction approach. This model architecture is similar to SimCLR except that it utilises only positive pairs, and the loss is calculated based on a cross-correlation matrix between the projections. BT shows competitive results with BYOL on certain aspects, such as batch size and asymmetry requirements, but BT networks are not robust toward augmentation and require higher projection output. Although this network trains well with a smaller batch size (1024) in comparison to BYOL, this still requires us to train both sides of the network. This ultimately makes it more computationally costly, where hardware availability is still a constraint.

While continuous improvement has been seen in the architectures of SSL networks, this area is still being explored thoroughly, with efforts focusing on examining each network layer, the usefulness of stop gradient in collapsing, and investigation of appropriate loss functions. As all network performances fluctuate across different datasets and with different parameters and network settings, it is not yet possible for us to determine which of these models ultimately performs best.

B. SSL and Remote Sensing

Due to the lack of available labelled data in the remote sensing (RS) domain, and the gap which exists with non-RS RGB images in terms of spectral and spatial context, work in the RS domain is now leveraging self-supervised learning to pre-train RS based models for downstream tasks.

Recent literature has shown the popularity of applying both pre-text tasks (PTT) and contrastive learning methods. The work by Vincenzi et al., [10] utilises colourisation as their pre-text task to learn spectral information by utilising multi-spectral images. Meanwhile, work by Tao et al., applies instance discrimination based PTT to RGB remote sensing data, which performs well on downstream tasks with small datasets [22].

Some works utilise contrastive learning with the application of MoCo based models to temporal [23] and spatially augmented RGB remote sensing images [11]. SeCo [20] is one such approach, which utilises the MoCo architecture with multi-augmentation contrastive learning method by taking account of seasonal contrast in RGB remote sensing data. Also, quite a few works have attempted to fully exploit both sensor modalities, i.e., multi-spectral and SAR images, for representation learning with contrastive or distillation networks. One such work utilises contrastive multi-view coding

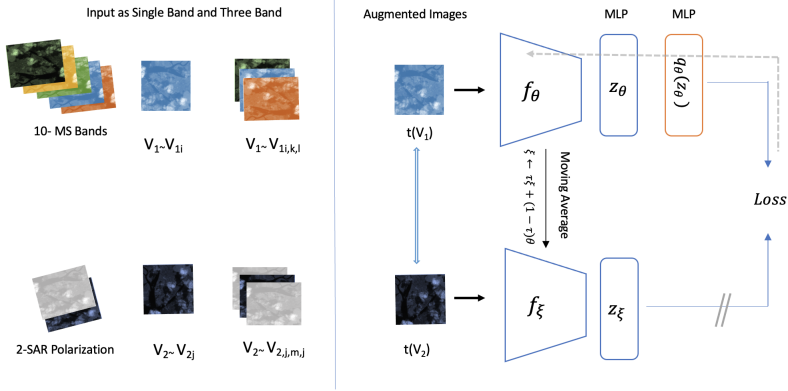


Fig. 1: Model architecture consist of an Encoder (f), a MLP projection head (z), and a MLP prediction head ($q(z)$). Input images do not represent actual band here but used only for multiple band representation.

(CMC) by leveraging multiple high and low resolution remote sensing datasets [4]. Chen & Bruzzone shows the use of both modalities using contrastive loss for pixel-level learning [2]. Another work by Chen & Bruzzone, concatenates MS and SAR temporal images to obtain pixel-level discrimination embedding with the distillation network for change detection [24]. Meanwhile, work by Jain et al., demonstrates that single channel features can also provide significant advantages in learning invariant representations for satellite data [3]. Similar results are shown by Montanaro et al. [25], which uses a combination of contrastive learning and the text task with the single-channel feature learning. Though it has been seen that similarity-based networks such as SimSiam do not perform well in the case of remote sensing [3], [25], we believe that distillation networks provide extra advantages for the learning of invariant spectral and spatial representations.

In addition, all these works highlighted the benefit of learning RS based representations for other downstream tasks rather than utilising RGB natural image based pre-trained models. Moreover, it has been established that SSL provides a solution to the problem of large labelled data without compromising the performance compared to supervised learning. This motivated us to provide better experimental analysis on self-supervised distillation networks for RS representation learning by utilising both MS and SAR data.

III. METHODOLOGY

This section presents our framework for multi-modal satellite image representation learning based on distillation networks in self-supervised learning. This framework builds on the concept of distillation networks, and in particular, the BYOL architecture, but adopts a particular strategy to the application and training process for multi-modal data.

Self-supervised learning is based on the weak smoothness assumption, which states that distortion or adding perturbation to an image do not change its labels [26]. This work revolves around the same concept with multi-view representation similarity. To put this another way, since MS and SAR images are two views of the same location, our modelling leverages the implication that having different sensor images does not change the images' geographical properties.

Let us assume that MS and SAR images are in practice two views V_1 and V_2 , and that $f(V)$ is a representation of a view. The goal of this work is then to increase the similarity between the representations of the two views, say:

$$f(V_1) \Leftrightarrow f(V_2)$$

As indicated, the most appropriate network for such learning is arguably the siamese networks due to the duality of the data. However, the trivial solution to siamese networks is prone to collapse to constant representations, which led to the rise of contrastive and distillation networks.

Considering our goal is to learn invariant representations from MS (V_1) and SAR (V_2), we trained a remote sensing network (RSDnet) based on the BYOL architecture. The architecture follows the Student-Teacher type asymmetry, where students and teachers have identical encoders ($f(T(V))$). Moreover, weights are updated only for the student side of the network, whereas teacher network weights are modified based on the moving average of student weights. In order to add more asymmetry to the network, an extra predictor, i.e. a multi-layer perceptron (MLP) head, has been added to the student side of the network. The network compares L2 normalised prediction from student and teacher sides of the network, which is an output of a predictor head ($q(z)$) and projection head (z) respectively. The projection and prediction heads are 2-layer multi-layer perceptron (MLP) of hidden projection size 256 with batch normalisation and a non-linear (ReLU) layer.

The loss is calculated between the L2 normalised prediction head output $q(z_\theta)$ from the student side and projection head output z_ξ from the teacher side. Here θ is the weight of the student network, ξ is the weight of the teacher network, which is an exponential moving average of θ . As shown in Eq 1, ξ is updated by θ and the decay rate (τ), which in this network is 0.9.

$$\xi \leftarrow \tau \xi + (1 - \tau) \theta \quad (1)$$

This implicitly provides asymmetry and prevents the model from learning the same latent representations, which in turn prevents collapse.

The loss function for the network is represented as in Eq 2, where $\|\cdot\|_2$ is L_2 normalisation, and t and t' are the augmentation applied to views V_1 and V_2 :

$$L(t(V_1), t'(V_2)) = 2 - 2 \cdot \frac{q(z_{\theta,1})}{\|q(z_{\theta,1})\|_2} \cdot \frac{z_{\xi,2}}{\|z_{\xi,2}\|_2} \quad (2)$$

Our loss function is the mean square error (MSE) between the two projections for the augmented views of the MS and SAR images. Total loss is calculated by interchanging views between the student and teacher network, which results in the total MSE as in Eq 3.

$$Loss_{total} = L(t(V_1), t'(V_2)) + L(t'(V_2), t(V_1)) \quad (3)$$

This architecture not only prevented the collapsing issue, but also provides better performance than some of the contrastive learning approaches and helped reduce the batch size requirement for training. While this architecture performs well, many research works have shown different analyses such as the use of the batch normalisation layer do not help in avoiding collapse [27], but rather that stop gradient is the key to avoid collapse [28]. In other words, these works show that there is still a need for more analysis in terms of the reasons for the outstanding performance of BYOL like distillation networks and further need to explore them in other domains such as remote sensing.

In order to better understand the representation learnt from the RS data, we pre-trained our models into two variants: (i) a single-channel model and (ii) a three-channel model. For the single channel model, two views were randomly selected from MS and SAR bands, that is one MS band (V_{1i}) out of 10 bands, i.e. $i = \{1, 2, \dots, 10\}$, and one SAR polarisation (V_{2j}), i.e. $j = \{1, 2\}$. On the other hand, the three-channel model utilises the same approach except that it draws upon a random three bands from the MS data and generates three-channel SAR images by randomly copying a third channel from the two polarisations. These two views are then randomly augmented with transformations t and t' before sending them to the encoder.

After pre-training of the model, MLP heads are removed, and we use only student encoder weights for the downstream task, which in our case, we evaluate on different remote sensing datasets.

This work demonstrates the usefulness of RSDnet, which is trained to learn single and three channel RS-based invariant features. We compare our work with random initialisation, ImageNet & MS COCO pre-trained ResNet50, and SeCo [20] weights to explore the usefulness of RSDnet models against models trained with non-RS data and RS-based contrastive model.

IV. EXPERIMENT

In this section, we discuss the implementation details of the RSDnet models and give details on datasets and data augmentation used.

A. Datasets

We pre-trained our models with the Sen12MS dataset, which consists of 180,000 pairs of Sentinel-1 and Sentinel-2 images of size 256 x 256 pixels. Where Sentinel-1 (SAR) has VV and

VH polarisation, Sentinel-2 has 13 multi-spectral (MS) bands. Among the 13 MS bands, in this work, we used 10 bands of 10m-20m resolution and discarded three atmospheric bands of 60m resolution. We utilised 50% of the data for our work – that is 90K pairs of images. The reason for using 50% data is due to the hardware limitation as larger dataset adds the computational cost.

For evaluation of the representations learned by the models, we utilised two benchmark datasets for a land cover classification task, i.e., EuroSAT [29] and RESISC45 [30]. EuroSAT consists of 64 x 64 size images and is similar to Sen12MS in terms of sensor and spectral information. It consists of 10 land cover classes with 27,000 images. Meanwhile, the RESISC45 dataset consists of high-resolution RGB images of size 256 x 256 pixels and contains 31,500 images, covering 45 scene classes. We also evaluated our models on 5000 images from Sen12MS.

Finally, we utilised the IEEE Data Fusion Contest (DFC) 2020 land cover mapping dataset for segmentation evaluation, which is a subset of Sen12MS data and contains 12,228 pairs of labelled Sentinel-1/2 data. Of these, we used 900 images for the linear evaluation. The dataset consists of 10 land cover classes based on the IGBP classification scheme. Among the 10 classes, we excluded “Savanna” and “Snow/Ice” as these classes are rare in this subset of Sen12MS and utilised 8 land cover classes, that is, forest, scrubland, grassland, wetlands, croplands, urban / built-up, woodland, and water.

B. Data Augmentation

We used all augmentation techniques applied in [18] apart from colour jitter, as this work implicitly applies colour jitters to images through the use of Random MS and SAR bands. We also utilised random pixel erasing to provide stronger augmentation to the images. Thus, our augmentations include random flips, rotation, Gaussian blur, random pixel erasing, and resized crops with bicubic interpolation. We also applied random greyscale to three band images.

C. Experimental Settings and Parameters

For pre-training the model, we utilised ResNet50 as the backbone encoder and the SGD optimiser with a cosine warm restart scheduler. The warm restart of 10 epochs was given with a multiplier of 2, and the learning rate ranges between 0.002 and 0.2. We utilised a batch size of 32 and trained all our models for 400 epochs with weight decay of 1e-5.

The following subsections explain individual settings and variations for single channel and three channel model variants.

1) *Single Channel Models*: For single channel feature learning, RSDnet-1 was trained with random bands from MS as view V_1 and a random selection of VV and VH from SAR as view V_2 .

We trained RSDnet-1 in multiple variations to look at the impact of each RSDnet’s representation learning. These variations were: (i) increasing batch size, (ii) increasing dataset size, and (iii) utilising only the multi-spectral dataset.

Most of the best performing SSL networks such as BYOL, Dino, MoCo utilise much larger batch sizes than 32 to attain

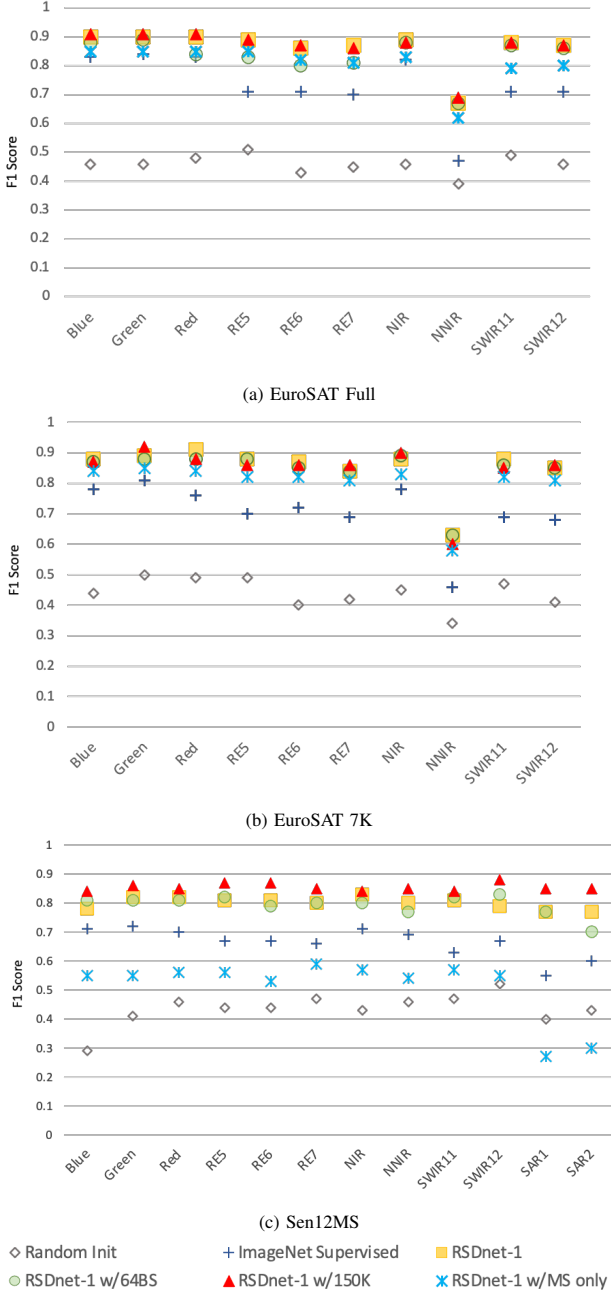


Fig. 2: Band-Wise Linear Evaluation for Single Channel Models on EuroSAT and Sen12MS Datasets

the maximum performance, thus we also trained RSDnet-1 with 64 batch size. This variation was made to analyse the impact of batch size on feature learning. As our dataset is not as large as those datasets that typically large networks are trained on, making use of a large batch size would likely not be a benefit for RSDnet-1 in practice. This upper batch size of 64 was influenced by our hardware limitations.

Further, we analysed the impact of training with different dataset sizes on RSDnet-1. For this training, we increased the dataset size by 30% by utilising 150K pairs from Sen12MS.

Finally, to better understand the usefulness of SAR data in learning invariant representation, we also trained our model with single modality, i.e. MS data only. This study examines

the benefit of using multi-sensor data for remote sensing representation learning.

Each of these variations were trained with the same architectural and parameter settings, i.e., encoder, optimiser, scheduler, epochs, and batch size, except for the case of the 64 batch size variation.

2) *Three Channel Models*: For the three-channel remote sensing based feature learning model, we utilised two different input techniques. The first technique RSDnet-3 is similar to our single-channel model (RSDnet-1), which takes three random MS bands as one view (V_1) and SAR's VV & VH bands as another view (V_2); we copied the third channel randomly for the third SAR view. Another input technique which we applied is *RGB-SIS2*, which keeps one view (V_1) as red, green, and blue bands (RGB) and another view (V_2) with one SAR and two random non-RGB MS bands such as red edge, narrow infrared, or shortwave infrared bands.

We utilised a single Nvidia RTX 2080Ti GPU for pre-training and evaluation of the models ¹.

V. EVALUATION

For the evaluation of RSDnet's learned representations, we performed a linear evaluation. That is, we froze encoder weights and added a simple linear classifier head. The classifier head was a MLP with a hidden dimension of 128, followed by batch normalisation layers, ReLU, and a softmax layer. We trained all the model variants for 100 epochs and utilised cross-entropy loss as our loss function. For downstream classification tasks we compared our RSDnet weights with random initialisation and ImageNet pre-trained weights for both single channel and three channel models. We also compared three channel RSDnet weights with SeCo weights, which are trained on 1 million RGB remote sensing images with a contrastive learning architecture.

Additionally, in order to evaluate how well representations learned pixel level information, we also provided an evaluation on land cover mapping with the DFC 2020 Sen12MS dataset. Both single and three channel RSDnet utilised the DeepLabV3 model architecture with a ResNet50 encoder. As was the case with linear evaluation, we froze the weights of the encoder and trained only the decoder. We also compared our three channel RSDnet weights with an MS COCO trained on DeepLabV3 and SeCo weights to analyse the benefit of using multi-modal MS and SAR data learning with a SSL distillation network.

A. Single Channel Models

Figure 2 shows the F1 score of the band-wise evaluation on the EuroSAT Full, EuroSAT 7K, and Sen12MS 5K datasets. To evaluate the ImageNet derived model, we copied single band information into three channels, which is the standard solution available for greyscale or single band data. It is evident that RSDnet-1 and RSDnet-1 w/150K has almost similar performance, but RSDnet-1 w/150K outperformed all other versions on EuroSAT full and Sen12MS 5K datasets. Especially in the SAR bands, the gap between RSDnet-1 w/150K and other versions is quite significant.

¹Code and trained models will be publicly available if accepted.

TABLE I: Channel-wise Linear Evaluation on DFC Segmentation Dataset

Band		Blue	Green	Red	RE5	RE6	RE7	NIR	NNIR	SWIR1	SWIR2	SARI	SAR2	Average
RSDnet-1	mIoU	54.8	57.7	57.8	58.3	54.5	56.6	57.6	55.5	58.1	58.5	57.2	57.2	56.98
	AA	68.0	72.2	70.7	72.1	68.2	69.7	70.8	68.4	71.4	72.3	70.1	70.5	70.38
RSDnet-1 w/150K	mIoU	54.3	58.6	57.6	57.6	56.4	56.6	57.6	55.3	57.6	57.9	57.5	57.5	57.05
	AA	71.0	72.1	73.0	70.7	69.8	69.6	71.2	67.9	70.6	71.5	71.2	71.8	70.87
RSDnet-1 w/64BS	mIoU	57.7	59.6	58.8	59.1	57.5	54.8	56.0	56.5	59.2	58.4	58.3	57.8	57.81
	AA	72.0	72.7	72.5	73.1	71.3	68.0	69.6	69.6	72.4	72.0	70.9	71.2	71.27

With these results, it can be seen that models trained in a supervised fashion with a large amount of data, such as ImageNet, show average performance. At the same time, a slight increase in remote sensing data lead to a competitive result. This opens the possibility of better representation learning in the remote sensing domain with larger datasets in a self-supervised fashion. However, the performance for a subset of EusoSAT, that is, EuroSAT 7K, shows different results, as RSDnet-1 outperforms RSDnet-1 w/150K with a performance gap of 1-3% for most bands. To better understand if these results are significant, we also performed a t-test for the EuroSAT results, but found no significant difference between RSDnet-1 and RSDnet-1 w/150K. This emphasises that in terms of computational cost and performance, RSDnet-1 still outperforms all other versions.

As noted earlier, while BYOL and similar architectures show the best performance when trained with a very large batch size such as 4096, we only utilised a batch size of 32 due to hardware limitations. However, we also trained RSDnet-1 on a batch size of 64 to evaluate the potential impact of increasing batch sizes. However, with increased batch size the results did not improve compared to RSDnet-1 with a batch size of 32. This could be due to the small size of our training datasets in contrast to the original models trained on ImageNet. Despite the small dataset, all our single-channel versions outperformed the ImageNet trained ResNet50 models. These results predominantly demonstrate the usefulness of RS based pre-trained models.

RSDnet-1 trained only on MS data did not show good results compared to our MS-SAR models. In addition to that, the results with SAR bands show extreme under performance, which indicates the usefulness of multimodality for pre-training. A t-test evaluation shows p-value<0.05 for *RSDnet-1 MS only* with all other variations, which indicates the significant difference in the overall performance. We speculate that the reason for this may be due to spectral augmentation alone in remote sensing not helping the SSL model to learn invariant representations compared to using MS-SAR data.

Regarding ImageNet results, it can be seen that bands with higher resolution (10m), i.e. Red, Green, Blue and NIR, have a smaller gap in performance using RSDnet-1, whereas bands with the lower resolution of 20m or SAR images show a more significant gap in performance using RSDnet-1. This further confirms the usefulness of RS pre-trained models.

Table I illustrates that, for pixel-level information, increased batch size does aid performance. This can be seen in the mean intersection over union (mIoU) and Actual Accuracy (AA) of each multi-spectral band. However, the overall difference in results with other model versions is not very large. These

results also reveal that the model performs well in both SAR and MS data, as the SAR results are also competitive with MS data. It also needs to be taken into account that these results are highly skewed due to water class detection. The accuracy of the water pixels is around 90% and above for all bands in the DFC 2020 dataset. This can be seen in Figure 3, as water classes are predicted well by all three variations of RSDnet-1 for NNIR and SWIR bands. This can be assumed to be due to bands' reflection property as NNIR and SWIR are both able to detect water pixels more profoundly. Meanwhile, class-wise performance analysis on each band in Figure I shows that almost all bands show good results for water pixels as compared with other classes. Also notably, almost all bands show similar performance for each class including SAR bands.

B. Three Channel Models

Table II presents the F1 score of our three-channel model evaluation on EuroSAT Full, EuroSAT7K, Sen12MS and RE-SISC45 datasets. We compared RSDnet-3 weights with the ImageNet trained ResNet50 and SeCo weights. For all three datasets, we evaluated RSDnet-3's on typical red, green and blue (RGB) bands, and for non-RGB bands, we utilised Red Edge bands, i.e. RE5-RE6-RE7 and SAR (VV-VH-VV) bands in the Sen12MS dataset.

TABLE II: Linear Evaluation for a Three-Channel Model with RGB and Non-RGB Bands

Weights	EuroSAT 7K			EuroSAT Full			Sen12MS			RESISC45		RESISC45 95H
	RGB	RE5,6,7	RGB	RE5,6,7	RGB	RE5,6,7	SAR	RGB	RGB	RGB	RGB	
Random Init	0.46	0.44	0.50	0.45	0.40	0.49	0.27	0.36	0.27			
ImageNet Supervised	0.88	0.87	0.91	0.88	0.77	0.77	0.64	0.90	0.85			
SeCo [20]	0.90	0.85	0.92	0.88	0.81	0.80	0.68	0.88	0.82			
RSDnet-3	0.88	0.88	0.90	0.90	0.82	0.85	0.83	0.86	0.74			
RSDnet-3 RGB-S1S2	0.84	0.80	0.86	0.81	0.65	0.62	0.53	0.68	0.62			

TABLE III: Linear Evaluation of the three-channel model with RGB and non-RGB bands in the DFC segmentation dataset.

Three Bands	MS COCO (Supervised)		RSDnet-3		RSDnet-3 RGB-S1S2		SeCo [20]	
	mIoU	AA	mIoU	AA	mIoU	AA	mIoU	AA
RGB	48.6	63.6	51.6	66.9	49.7	64.1	49.0	64.1
RE5/6/7	46.2	61.5	51.3	65.8	46.2	61.8	49.8	64.5
SAR1/2/1	44.2	59.9	51.6	65.5	44.0	58.5	49.4	64.1

The results show that the ImageNet supervised and SeCo weights perform better for RGB images than our RS-based model except in the case of the Sen12MS dataset, where RSDnet-3 performed better. The good performance of ImageNet and SeCo on RGB images is not particularly surprising, as they are predominantly trained on large RGB image datasets. However, for non-RGB based images such as RE5/6/7 and SAR, RSDnet-3 performs the best. This emphasises the need for RS-specific models where data are typically not RGB images but MS or SAR images. In fact, it

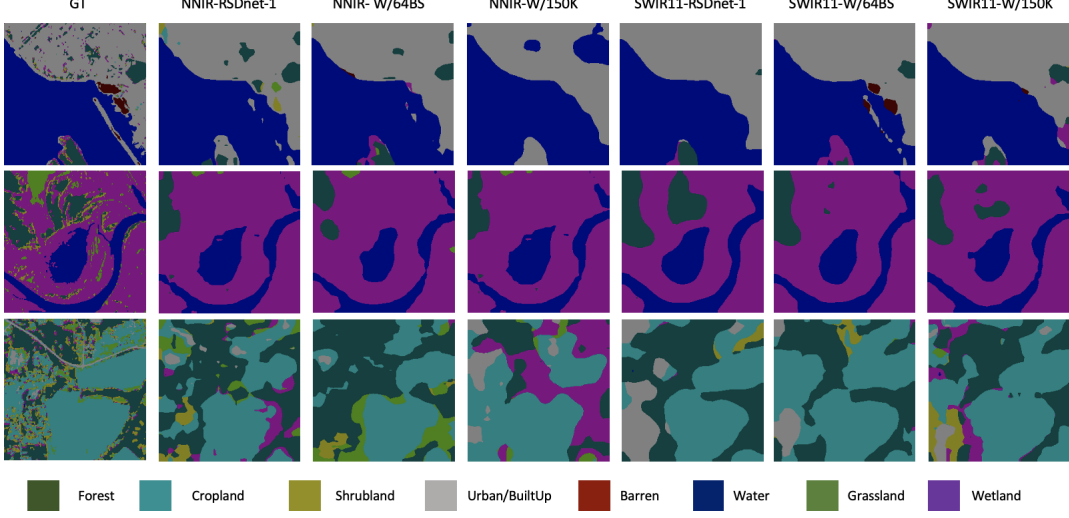


Fig. 3: DFC Segmentation linear evaluation prediction for single channel model with NNIR and SWIR11 band. Results are skewed due to higher water pixel in the data.

is notable that while ImageNet based models outperformed the RS based model for RGB images, the difference in results was not statistically significant and could potentially be reduced with further research on self-supervised learning.

In the case of RESISC45, the performance gap between ImageNet supervised and RSDnet-3 weights is due to the very high-resolution RGB data, whereas our RSDnets are trained with low-resolution data. This particularly applies to SeCo as well, as their trained weights are also based on low-resolution Sentinel-2 data. However, SeCo does perform better than RSDnet. This evaluation suggests that SSL type learning requires more research to generalise the models across the RS domain. One solution to such a problem is to utilise both low- and very high-resolution data for pre-training, which is also proposed by Stojnic et al. [4].

We argue that the under performance of *RSDnet-3 RGB-SIS2* demonstrates that randomisation of the spectral and SAR information provides better representation learning than using prominent MS data alone with the SSL distillation network.

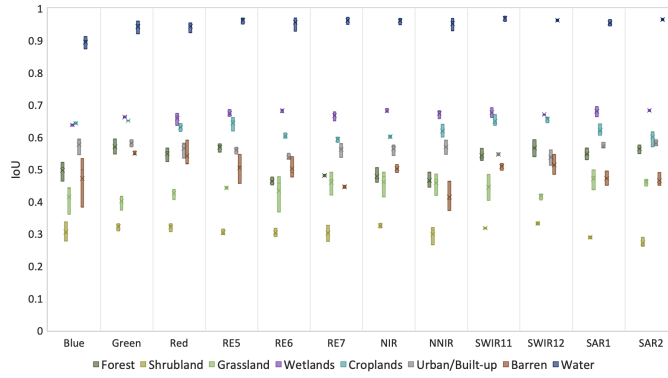


Fig. 4: Class wise performance boxplot on each band across single-channel RSDnets.

Further to our evaluation on pixel level learning by three channel models, Table III shows the results for *RSDnet-3* and *RSDnet-3 RGB-SIS2*. Similar to our classification evaluation, we also compared our results with an MS COCO pre-trained

model. Unlike in the classification task, the segmentation results for *RSDnet-3* and *RSDnet-3 RGB-SIS2* outperformed the MS COCO-based models. However, SeCo outperformed the weights of *RSDnet-3 RGB-SIS2* and MS COCO, yet *RSDnet-3* showed better results than SeCo. This further validates our hypothesis on usefulness of multi-modal training in comparison to single-modal learning. The results for the segmentation remained consistent for RGB and non-RGB satellite images.

The classification and segmentation results for the single-channel models in Figure 2 and Table I report competitive performance compared to any three channel feature learning weights in Tables II and III, including models pre-trained on ImageNet and MS COCO and SeCo weights. Based on these results, we argue that single bands can also provide good invariant representations in remote sensing compared to the popular notion of having a model with three or more bands.

VI. DISCUSSION

This work proposes RSDnet which utilises the SSL distillation architecture (BYOL) in the RS domain with the use of multi-modality, that is, MS and SAR data. We found that multi-modality enhances the performance of SSL based learning due to the stronger variance in data which makes representations more invariant. The results also show that when random MS and SAR bands are utilised for single channel feature learning, it can provide competitive results compared to common notion of three channel feature learning.

The efficiency of the RSDnets are further validated by the t-SNE plots in Figure 6 for 10 classes of the EuroSAT 7K dataset. We compared the feature embedding from ImageNet, SeCo, *RSDnet-3* and *RSDnet-3 RGB-SIS2* on RE5-6-7 band images. For single channel RSDnets feature embedding, we utilised RE5 band images. It can be seen that, RSDnets trained with the multi-modal approach form nice tight clusters in the embedding space compared to ImageNet and SeCo variants. However, SeCo shows better clustering than ImageNet, which further shows the benefit of using RS based data with SSL

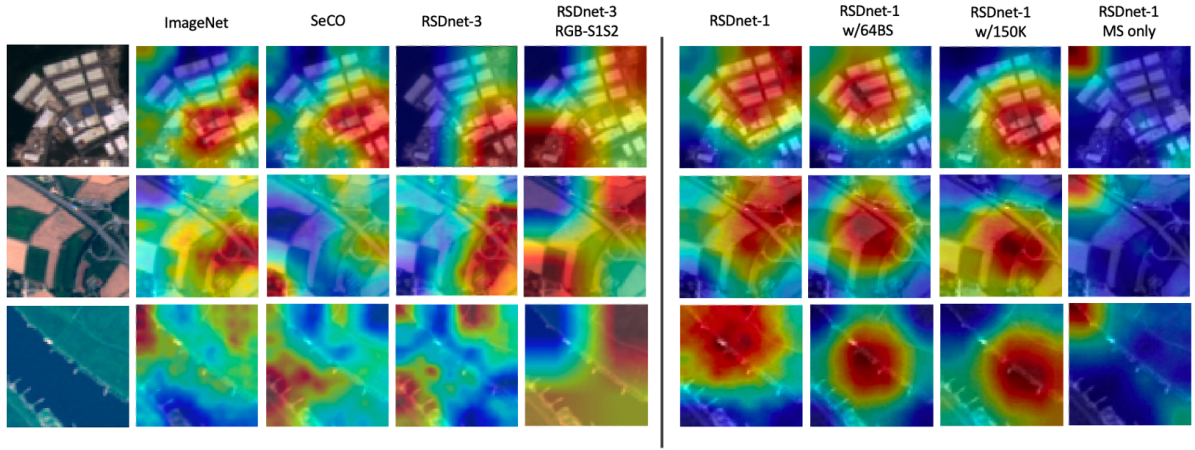


Fig. 5: Gradient class activation maps [31] for RSDnets and ImageNet pre-trained ResNet50. EuroSAT RGB images are used for three channel models, whereas Blue band image utilised for single channel models. Top, middle, and bottom row focuses on Industrial, Highway and River classes respectively.

types of learning. In addition to this, it can be seen that RSDnets trained with MS dominant data did not form clean clusters on embedding. This under performance suggests that in order to learn invariant representation in low resolution data, it is advantageous to leverage multiple modalities.

We also looked at the full gradient class activation maps (CAM) to understand where RSDnets, SeCo and ImageNet weights focus for class prediction in EuroSAT RGB and Blue band images. In Figure 5, it can be seen that single channel feature embedding strongly focuses on class specific regions along with the semantic separation between two classes such as river and land area. However, CAM for single-modality *RSDnet-1 MS only* shows out of region focus, which aligns with under performance for classification and segmentation tasks. Similar analysis can be seen in three channel MS dominant models, i.e. *RSDnet-3 RGB-S1S2*, which shows that while making decision, its region of focus is spread across the image.

The CAM for ImageNet, SeCo, and RSDnet-3 weights on river class are distributed across the image and also generally fail to find the stronger region of focus. For industrial classes, all three weights have stronger focus on smaller region of class despite the fact that 90% of the image covers the class. Whereas, in contrast it should be noted that the same model is very precise for the highway class for ImageNet and RSDnet-3. While these are illustrative examples, we believe such analysis can provide insights into the learning process.

Both single channel and three channel RSDnets performed well in downstream classification tasks, but need to improve at segmentation tasks at least in the case of three channel RSDnets. It should be noted however that we did not evaluate these with a fine tuning process, which might provide performance enhancement. This limitation can be further explored in the future to provide generalised network weights.

Finally, we note that RS-based SeCo showed competitive results with RSDnets, which shows the potential of SSL approaches in the RS domain to overcome the scarcity of labelled data. However, we argue that, in terms of computational efficiency, the BYOL based RSDnets are more efficient than a

contrastive learning based. This is due to the fact that training with BYOL style networks require only positive pairs, and use of stop gradient, which in return requires less batch size and memory requirements without compromising the performance.

VII. CONCLUSION

In this work, we applied the distillation network concept to build and analyse single channel and three channel feature learning for MS and SAR data. MS and SAR data provide implicit augmentation with spectral and structural information differences. This work showed that using MS and SAR as different views for network training provides better representation learning than utilising MS data alone.

We also showed that RS domain-based learning provides better results than non-RS based learning by comparing our results with results based on natural RGB datasets, such as ImageNet and MS COCO pre-trained models. Even though we trained our RSDnet with only 90K instances, in comparison for example with ImageNet (14 million), MS COCO (328K) dataset or SeCo (1 million), we achieved competitive results even with single channel feature learning alone. Another noticeable aspect of RSDnets is that, we trained the network with only 32 batch size unlike other networks trained on 256 or more. This may open the path for further research work in satellite data aiming to achieve better generalisation across the domain.

In continuation of our work, we will further explore other computationally efficient SSL networks and other RS-based pre-trained networks. Additionally, we would like to evaluate our models on further RS based datasets in order to better understand the learned representations.

VIII. ACKNOWLEDGEMENT

This research was conducted with the financial support of Science Foundation Ireland under Grant Agreement No. 13/RC/2106_P2 at the ADAPT SFI Research Centre at Technological University Dublin. ADAPT, the SFI Research Centre for AI-Driven Digital Content Technology, is funded by Science Foundation Ireland through the SFI Research Centres Programme.

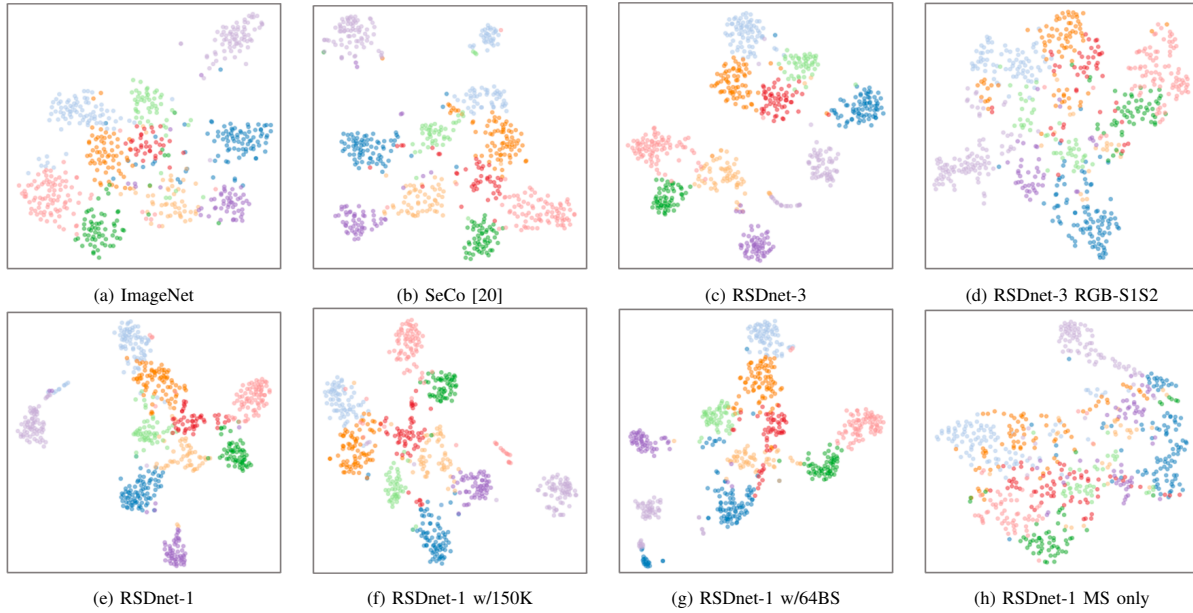


Fig. 6: T-SNE plot for EuroSAT RE5 band for single channel RSDnet's and RE5/6/7 bands for three channel RSDnets along with ImageNet (Supervised) and contrastive learning based remote sensing (SeCo) model [20]. The Red-Edge (RE) bands are utilised to show the impact of the model on non-RGB bands

REFERENCES

- C. Persello, J. D. Wegner, R. Hansch, D. Tuia, P. Ghamisi, M. Koeva, and G. Camps-Valls, “Deep learning and earth observation to support the sustainable development goals: Current approaches, open challenges, and future opportunities,” *IEEE Geoscience and Remote Sensing Magazine*, 2022.
- Y. Chen and L. Bruzzone, “Self-supervised sar-optical data fusion of sentinel-1/-2 images,” *IEEE Transactions on Geoscience and Remote Sensing*, 2021.
- P. Jain, B. Schoen-Phelan, and R. Ross, “Multi-modal self-supervised representation learning for earth observation,” in *2021 IEEE International Geoscience and Remote Sensing Symposium IGARSS*. IEEE, 2021, pp. 3241–3244.
- V. Stojnic and V. Risojevic, “Self-supervised learning of remote sensing scene representations using contrastive multiview coding,” in *Proceedings of the IEEE/CVF Conference on Computer Vision and Pattern Recognition*, 2021, pp. 1182–1191.
- Y. Li, J. Ma, and Y. Zhang, “Image retrieval from remote sensing big data: A survey,” *Information Fusion*, vol. 67, pp. 94–115, 2021.
- R. Pires de Lima and K. Marfurt, “Convolutional neural network for remote-sensing scene classification: Transfer learning analysis,” *Remote Sensing*, vol. 12, no. 1, p. 86, 2019.
- H.-C. Shin, H. R. Roth, M. Gao, L. Lu, Z. Xu, I. Nogues, J. Yao, D. Mollura, and R. M. Summers, “Deep convolutional neural networks for computer-aided detection: Cnn architectures, dataset characteristics and transfer learning,” *IEEE transactions on medical imaging*, vol. 35, no. 5, pp. 1285–1298, 2016.
- J. Kim and C. Park, “End-to-end ego lane estimation based on sequential transfer learning for self-driving cars,” in *Proceedings of the IEEE conference on computer vision and pattern recognition workshops*, 2017, pp. 30–38.
- Y. Yuan and L. Lin, “Self-supervised pre-training of transformers for satellite image time series classification,” *IEEE Journal of Selected Topics in Applied Earth Observations and Remote Sensing*, 2020.
- S. Vincenzi, A. Porrello, P. Buzzega, M. Cipriano, P. Fronte, R. Cuccu, C. Ippoliti, A. Conte, and S. Calderara, “The color out of space: learning self-supervised representations for earth observation imagery,” in *2020 25th International Conference on Pattern Recognition (ICPR)*. IEEE, 2021, pp. 3034–3041.
- J. Kang, R. Fernandez-Beltran, P. Duan, S. Liu, and A. J. Plaza, “Deep unsupervised embedding for remotely sensed images based on spatially augmented momentum contrast,” *IEEE Transactions on Geoscience and Remote Sensing*, vol. 59, no. 3, pp. 2598–2610, 2021.
- N. Komodakis and S. Gidaris, “Unsupervised representation learning by predicting image rotations,” in *International Conference on Learning Representations (ICLR)*, 2018.
- M. Noroozi and P. Favaro, “Unsupervised learning of visual representations by solving jigsaw puzzles,” in *European conference on computer vision*. Springer, 2016, pp. 69–84.
- R. Zhang, P. Isola, and A. A. Efros, “Colorful image colorization,” in *European conference on computer vision*. Springer, 2016, pp. 649–666.
- I. Misra and L. v. d. Maaten, “Self-supervised learning of pretext-invariant representations,” in *Proceedings of the IEEE/CVF Conference on Computer Vision and Pattern Recognition*, 2020, pp. 6707–6717.
- T. Chen, S. Kornblith, M. Norouzi, and G. Hinton, “A simple framework for contrastive learning of visual representations,” in *International conference on machine learning*. PMLR, 2020, pp. 1597–1607.
- K. He, H. Fan, Y. Wu, S. Xie, and R. Girshick, “Momentum contrast for unsupervised visual representation learning,” in *Proceedings of the IEEE/CVF conference on computer vision and pattern recognition*, 2020, pp. 9729–9738.
- J.-B. Grill, F. Strub, F. Altché, C. Tallec, P. Richemond, E. Buchatskaya, C. Doersch, B. Avila Pires, Z. Guo, M. Gheshlaghi Azar *et al.*, “Bootstrap your own latent-a new approach to self-supervised learning,” *Advances in Neural Information Processing Systems*, vol. 33, pp. 21 271–21 284, 2020.
- M. Caron, H. Touvron, I. Misra, H. Jégou, J. Mairal, P. Bojanowski, and A. Joulin, “Emerging properties in self-supervised vision transformers,” in *Proceedings of the IEEE/CVF International Conference on Computer Vision*, 2021, pp. 9650–9660.
- O. Mañas, A. Lacoste, X. Giro-i Nieto, D. Vazquez, and P. Rodriguez, “Seasonal contrast: Unsupervised pre-training from uncurated remote sensing data,” in *Proceedings of the IEEE/CVF International Conference on Computer Vision*, 2021, pp. 9414–9423.
- J. Zbontar, L. Jing, I. Misra, Y. LeCun, and S. Deny, “Barlow twins: Self-supervised learning via redundancy reduction,” in *International Conference on Machine Learning*. PMLR, 2021, pp. 12 310–12 320.
- C. Tao, J. Qi, W. Lu, H. Wang, and H. Li, “Remote sensing image scene classification with self-supervised paradigm under limited labeled samples,” *IEEE Geoscience and Remote Sensing Letters*, 2020.
- K. Ayush, B. Uzkent, C. Meng, K. Tanmay, M. Burke, D. Lobell, and S. Ermon, “Geography-aware self-supervised learning,” in *Proceedings of the IEEE/CVF International Conference on Computer Vision*, 2021, pp. 10 181–10 190.
- Y. Chen and L. Bruzzone, “Self-supervised change detection by fusing sar and optical multi-temporal images,” in *2021 IEEE International Geoscience and Remote Sensing Symposium IGARSS*. IEEE, 2021, pp. 3101–3104.
- A. Montanaro, D. Valsesia, G. Fracastoro, and E. Magli, “Self-supervised learning for joint sar and multispectral land cover classification,” *arXiv preprint arXiv:2108.09075*, 2021.

- [26] J. E. Van Engelen and H. H. Hoos, “A survey on semi-supervised learning,” *Machine Learning*, vol. 109, no. 2, pp. 373–440, 2020.
- [27] P. Richemond, J.-B. Grill, F. Altché, C. Tallec, F. Strub, A. Brock, S. Smith, S. De, R. Pascanu, B. Piot *et al.*, “Byol works even without batch statistics,” in *NeurIPS 2020 Workshop: Self-Supervised Learning-Theory and Practice*, 2020.
- [28] X. Chen and K. He, “Exploring simple siamese representation learning,” in *Proceedings of the IEEE/CVF Conference on Computer Vision and Pattern Recognition*, 2021, pp. 15 750–15 758.
- [29] P. Helber, B. Bischke, A. Dengel, and D. Borth, “Eurosat: A novel dataset and deep learning benchmark for land use and land cover classification,” *IEEE Journal of Selected Topics in Applied Earth Observations and Remote Sensing*, vol. 12, no. 7, pp. 2217–2226, 2019.
- [30] G. Cheng, J. Han, and X. Lu, “Remote sensing image scene classification: Benchmark and state of the art,” *Proceedings of the IEEE*, vol. 105, no. 10, pp. 1865–1883, 2017.
- [31] S. Srinivas and F. Fleuret, “Full-gradient representation for neural network visualization,” *Advances in neural information processing systems*, vol. 32, 2019.